

Supporting Information

Highly Stable and Re-dispersible Nano Cu Hydrosols with Sensitive Size-dependent Catalytic and Antibacterial Activities

Yu Zhang,^{†a,b,c} Pengli Zhu,^{†*a} Gang Li,^a Wenzhao Wang,^a Liang Chen,^a Daoqiang Daniel Lu,^{*a} Rong Sun,^{*a} Feng Zhou^b and Chingping Wong^{d,e}

^a Shenzhen Institutes of Advanced Technology, Chinese Academy of Science, 1068 Xueyuan Avenue, Shenzhen University Town, Shenzhen, 518055, China, E-mail: pl.zhu@siat.ac.cn or rong.sun@siat.ac.cn

^b State Key Laboratory of Solid Lubrication, Lanzhou Institute of Chemical Physics, Chinese Academy of Sciences, Lanzhou, China

^c Shenzhen College of Advanced Technology, University of Chinese Academy of Sciences, Shenzhen, China

^d Department of Electronics Engineering, The Chinese University of Hong Kong, Hong Kong SAR, China

^e School of Materials Science and Engineering, Georgia Institute of Technology, Atlanta, USA

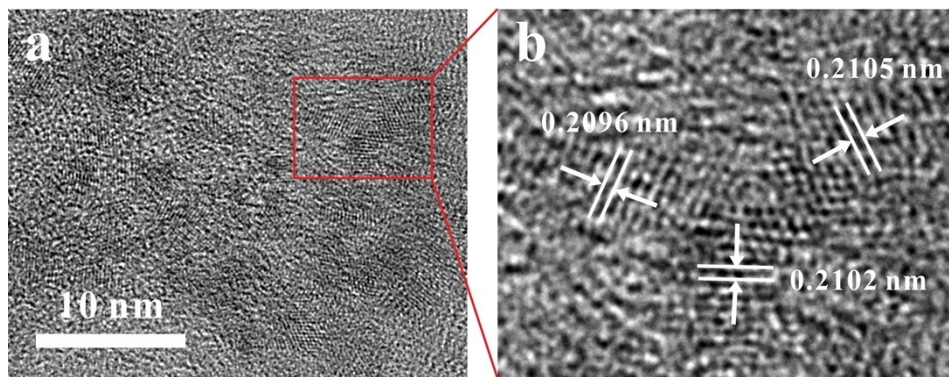


Fig. S1 HRTEM images of S1 with different magnifications.

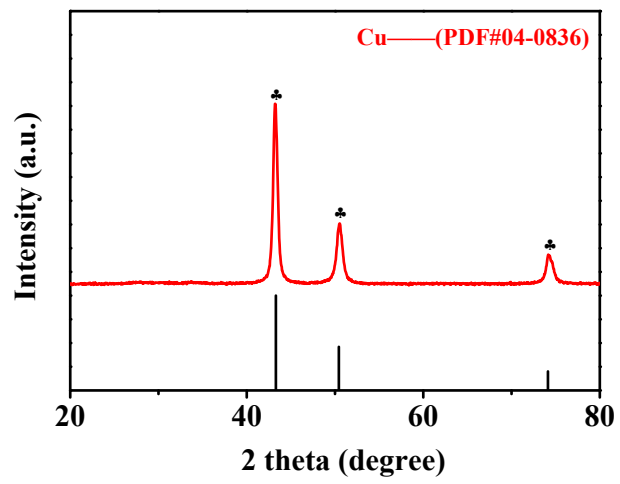


Fig. S2 XRD pattern of S6 after centrifugal washing.

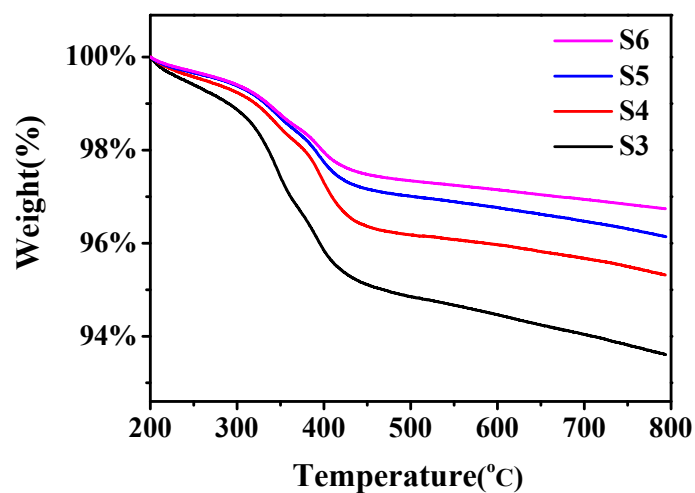


Fig. S4 TG results of samples S3-S6 after high-speed and long-time centrifugal washing under N₂ atmospheres.

TGA tests of the prepared samples S3-S6 after high-speed and long-time centrifugal washing have been carried out as shown in Fig. S4 (S1 and S2 are so small and stable in the mother liquid, it is difficult for us to get the centrifugal separations). The results show that the weight loss of samples (S3-S6) obviously decreases in the range from the room temperature to 800 °C under N₂ atmospheres. Combined with the other characterization results in the manuscript, it could be considered that from S3 to S6, the particle size increases, following with organics coating on the surface of single particle decreasing gradually. Therefore, after the heat treatment to 800 °C, the weight loss declines by degrees from S3 to S6. It is precisely because the different amount of polymer chains on the surface of each particle that resulting in the different size of copper nanoparticles. And the results are also consistent with the inferred growth mechanism.

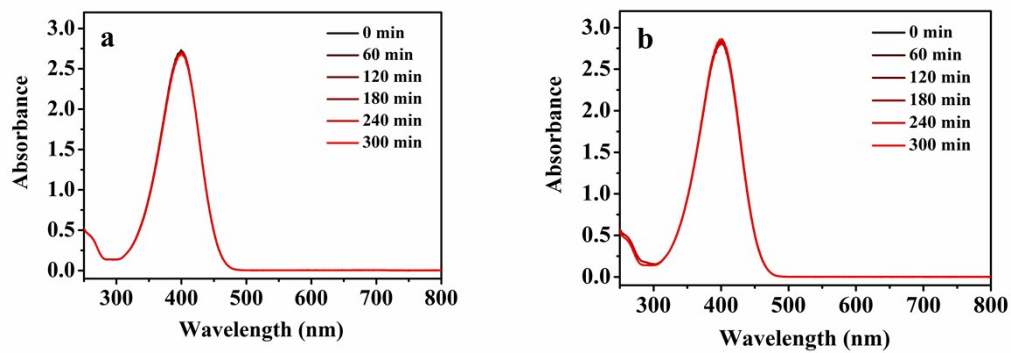


Fig. S5 UV-visible absorption spectra of catalytic reduction of 4-NP by NaBH_4 without catalyst (a) and with SO which only contains hydrosol organics without copper nanoparticles (b).

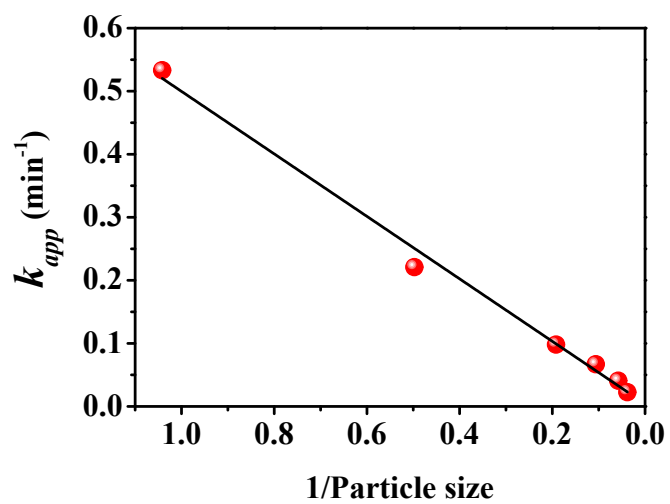


Fig. S6 The real relationship between k_{app} and the reciprocal of the particle size.

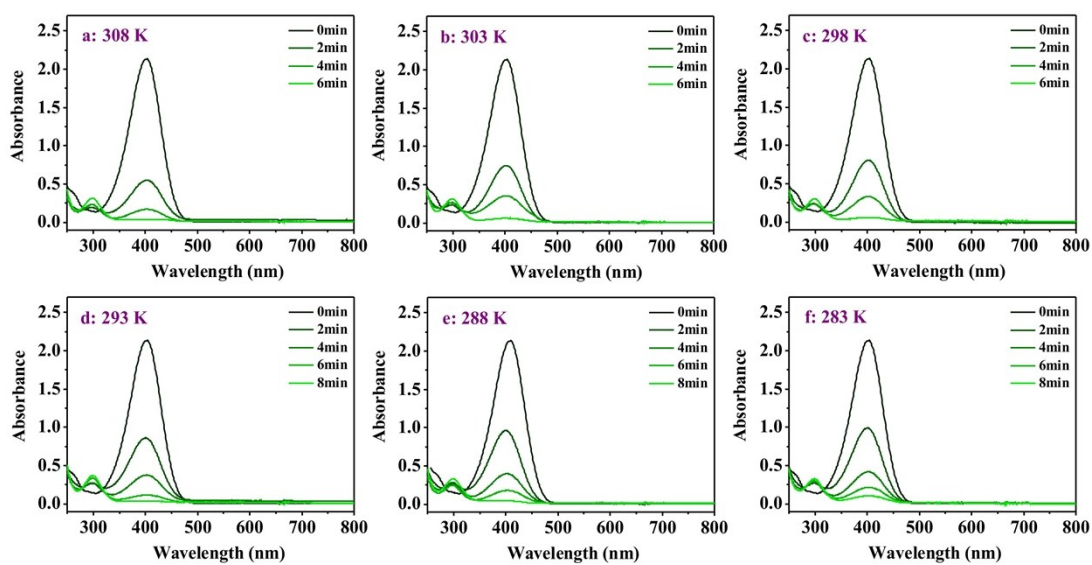


Fig. S7 UV-visible absorption spectra of catalytic reduction of 4-NP by NaBH₄ with S1 under different temperatures.

Table S1 Particle characteristics of the nano Cu hydrosols prepared at different concentrations of copper precursor and the resulted apparent rate constants k_{app} for catalytic reduction of 4-NP with NaBH₄.

No.	Concentration of precursor (mol)	Size of Cu hydrosol (nm)	Volume of using (μ l)	Quality of using ($\times 10^{-5}$ g)	Surface area of using (cm ²)	Apparent rate constants k_{app} (min ⁻¹)
S1	0.001	0.96	100.0	5.818	408.57	0.53331
S2	0.005	2.01	20.0	5.818	195.14	0.22089
S3	0.010	5.21	10.0	5.818	75.28	0.09815
S4	0.015	9.42	6.7	5.818	41.64	0.06693
S5	0.020	17.36	5.0	5.818	22.59	0.04082
S6	0.025	26.26	4.0	5.818	14.94	0.02252

Table S2 The resulted apparent rate constants k_{app} for catalytic reduction of 4-NP with S1 under different temperatures.

Kelvin temperature (K)	$1000/T$ (K^{-1})	k_{app} (min^{-1})	$\ln k_{app}$ (min^{-1})	R^2
308	3.24675	0.59246	-0.52347	0.9967
303	3.30033	0.56554	-0.56997	0.9973
298	3.35570	0.52273	-0.64869	0.9985
293	3.41297	0.49843	-0.69629	0.9948
288	3.47222	0.46158	-0.77310	0.9987
283	3.53357	0.42983	-0.84437	0.9988

Table S3 Comparison of activation energy E_a for catalytic reduction of 4-NP in our work and the relevant literatures with more details.

Ref.	Catalyst type	Dosage of catalyst	Concentration and dosage of 4-NP	Concentration and dosage of NaBH ₄	E_a (kJ mol ⁻¹)
Our work	Cu hydrosol	9.1 mM, 0.1 mL	0.2 mM, 30 mL	0.02 M, 10 mL	9.37
Gupta ²⁸ (Water Res.)	Fe@Au ATPGO	1.4 g L ⁻¹	0.1 mM, 25 μ L	0.06 M, 2.5 mL	9.75
Zhang ²⁹ (J. Mater. Chem. A)	Cu cubes	15 mM, 0.1 mL	0.1 mM, 1.7 mL	0.04 M, 0.7 mL	22.44
Yamamoto ³⁰ (Nanoscale)	Au nanoclusters	1 μ M	0.1 mM	0.2 M	31
Kalekar ³¹ (Langmuir)	Pt nanoballs	50 mg L ⁻¹ , 0.5 mL	0.1 mM, 1.5 mL	0.05 M, 1.0 mL	6.4
	Pt nanonets	50 mg L ⁻¹ , 0.5 mL	0.1 mM, 1.5 mL	0.05 M, 1.0 mL	26
Zeng ²³ (Nano Lett.)	Au-Based nanocages	3.8×10^9 particles mL ⁻¹	0.14 mM	0.042 M	28.04 \pm 1.43
	Au-Based nanoboxes	3.8×10^9 particles mL ⁻¹	0.14 mM	0.042 M	44.25 \pm 2.62
	Au-Based partially hollow nanoboxes	3.8×10^9 particles mL ⁻¹	0.14 mM	0.042 M	55.44 \pm 3.15
Mahmoud ²² (Nano Lett.)	Pt-Pd alloy nanocages	200 μ L colloid	2 mM, 250 μ L	0.06 M, 2.0 mL	109.67 \pm 7.53
	Pd nanocages	200 μ L colloid	2 mM, 250 μ L	0.06 M, 2.0 mL	94.60 \pm 6.28
	Pt/Pd nanocages	200 μ L colloid	2 mM, 250 μ L	0.06 M, 2.0 mL	77.44 \pm 5.44
	Pd/Pt nanocages	200 μ L colloid	2 mM, 250 μ L	0.06 M, 2.0 mL	86.65 \pm 7.53
	Pt nanocages	200 μ L colloid	2 mM, 250 μ L	0.06 M, 2.0 mL	67.81 \pm 4.60